

# Comparison of Two Methods for Obtaining Quantitative Mass Concentrations from Aerosol Time-of-Flight Mass Spectrometry Measurements

Xueying Qin, Prakash V. Bhave,<sup>†</sup> and Kimberly A. Prather\*

Department of Chemistry and Biochemistry, University of California, San Diego, 9500 Gilman Drive, La Jolla, California 92093-0314

Aerosol time-of-flight mass spectrometry (ATOFMS) measurements provide continuous information on the aerodynamic size and chemical composition of individual particles. In this work, we compare two approaches for converting unscaled ATOFMS measurements into quantitative particle mass concentrations using (1) reference mass concentrations from a co-located micro-orifice uniform deposit impactor (MOUDI) with an accurate estimate of instrument busy time and (2) reference number concentrations from a co-located aerodynamic particle sizer (APS). Aerodynamic-diameter-dependent scaling factors are used for both methods to account for particle transmission efficiencies through the ATOFMS inlet. Scaling with APS data retains the high-resolution characteristics of the ambient aerosol because the scaling functions are specific for each hourly time period and account for a maximum in the ATOFMS transmission efficiency curve for larger-sized particles. Scaled mass concentrations obtained from both methods are compared with co-located PM<sub>2.5</sub> measurements for evaluation purposes. When compared against mass concentrations from a beta attenuation monitor (BAM), the MOUDI-scaled ATOFMS mass concentrations show correlations of 0.79 at Fresno, and the APS-scaled results show correlations of 0.91 at Angiola. Applying composition-dependent density corrections leads to a slope of nearly 1 with 0 intercept between the APS-scaled absolute mass concentration values and BAM mass measurements. This paper provides details on the methodologies used to convert ATOFMS data into continuous, quantitative, and size-resolved mass concentrations that will ultimately be used to provide a quantitative estimate of the number and mass concentrations of particles from different sources.

Over the past two decades, the number of studies on airborne particulate matter has increased substantially due to increased awareness of the role of aerosols in reducing visibility, affecting climate change, and endangering human health.<sup>1–7</sup> Health risks

have been shown for particles with aerodynamic diameters <2.5  $\mu\text{m}$  (PM<sub>2.5</sub>), on the basis of mortality rates that show a positive correlation with particles in this size range.<sup>8</sup> Therefore, it is very important to perform regional-scale long-term monitoring to better understand the major sources impacting the annual PM<sub>2.5</sub> mass concentrations.

Although traditional off-line filter-based measurements are able to provide robust information on aerosol mass concentration and chemical composition, they still have limitations, such as low time resolution, sampling artifacts,<sup>9</sup> and very limited information on aerosol mixing state, which is essential for understanding the impacts of aerosols on climate and visibility.<sup>10</sup> Real-time single particle mass spectrometry (SPMS) measurements provide continuous on-line information on single particle size and chemical composition.<sup>11–13</sup> These measurements can be used to provide further insight into the associations between chemical species within individual particles, allowing one to link composition with specific sources and atmospheric processing. Particles are rapidly analyzed (<1 ms), minimizing the changes in particle morphology and the repartitioning of chemical species during the analysis. Despite these advantages, it has been a challenge for real-time SPMS instruments to provide quantitative information on aerosol mass concentrations. Several factors present obstacles in quantifying SPMS measurements. First, particle transmission efficiency is size-dependent and needs to be corrected using number concentrations from other co-located instruments.<sup>14</sup> Second, in most real-time SPMS methods, the ion signals in the mass spectra for identical particles can vary considerably from shot to shot due to inhomogeneities in the laser beam.<sup>15</sup> Third, instrument sensi-

\* Corresponding author. Phone: (858) 822-5312. Fax: (858) 534-7042. E-mail: kprather@ucsd.edu.

<sup>†</sup> Current address: Atmospheric Sciences Modeling Division, Air Resources Laboratory, National Oceanic and Atmospheric Administration, Research Triangle Park, NC 27711.

(1) Brunekreef, B.; Holgate, S. T. *Lancet* **2002**, *360*, 1233–1242.

(2) Horvath, H. *Atmos. Environ.* **1993**, *27*, 293–317.

(3) Jacobson, M. C.; Hansson, H. C.; Noone, K. J.; Charlson, R. J. *Rev. Geophys.* **2000**, *38*, 267–294.

(4) McClellan, R. O. *Ann. Rev. Pharmacol. Toxicol.* **1987**, *27*, 279–300.

(5) Oberdorster, G. *Int. Arch. Occup. Environ. Health* **2001**, *74*, 1–8.

(6) Robock, A. *Rev. Geophys.* **2000**, *38*, 191–219.

(7) Sydbom, A.; Blomberg, A.; Parnia, S.; Stenfors, N.; Sandstrom, T.; Dahlen, S. E. *Eur. Resp. J.* **2001**, *17*, 733–746.

(8) Pope, C. A. *Environ. Health Perspect.* **2000**, *108*, 713–723.

(9) Zhang, X. Q.; McMurry, P. H. *Atmos. Environ.* **1987**, *21*, 1779–1789.

(10) Heintzenberg, J. *Tellus* **1989**, *41(B)*, 142–160.

(11) Suess, D. T.; Prather, K. A. *Chem. Rev.* **1999**, *99*, 3007–3035.

(12) Noble, C. A.; Prather, K. A. *Mass Spectrom. Rev.* **2000**, *19*, 248–274.

(13) Johnston, M. V. *J. Mass Spectrom.* **2000**, *35*, 585–595.

(14) Dahneke, B. E.; Cheng, Y. S. *J. Aerosol Sci.* **1979**, *10*, 257–274.

(15) Wenzel, R. J.; Prather, K. A. *Rapid Commun. Mass Spectrom.* **2004**, *18*, 1525–1533.

tivities to different aerosol chemical species vary<sup>16,17</sup> and can change as a function of matrix composition<sup>18</sup> and particle size.<sup>19</sup> Fourth, when instrument operation and data acquisition are controlled by the same computer, the ability to detect incoming particles decreases with increasing ambient particle concentration due to instrument busy time.<sup>20</sup>

Due to the aforementioned issues, the quantitative potential of SPMS measurements has not been fully realized. A number of efforts have been dedicated to acquiring high temporal resolution quantitative information from SPMS data by scaling with co-located reference measurements.<sup>19–25</sup> Among the various SPMS instruments developed to date, most of the quantification efforts have been applied to aerosol time-of-flight mass spectrometry (ATOFMS), which acquires real-time information on single particle aerodynamic diameter ( $D_a$ ) and chemical composition. Although ATOFMS measures  $D_a$ , only Allen et al.,<sup>20,21</sup> Bhave et al.,<sup>19</sup> and Moffet et al.<sup>24</sup> have used  $D_a$ -based reference measurements to reconstruct quantitative results from ATOFMS data. Allen et al.<sup>20,21</sup> and Bhave et al.<sup>19</sup> used a micro-orifice uniform deposit impactor (MOUDI) as the reference method for quantification. Typical MOUDI measurements have a time resolution of ~5–8 h and a size resolution of 4 bins/decade. Moffet et al.<sup>24</sup> compared ATOFMS measurements against aerodynamic particle sizer (APS) measurements, which provide higher time and size resolution than the MOUDI, to obtain quantitative number concentrations.

In this paper, we compare both MOUDI scaling and APS scaling methods to quantify ATOFMS single particle measurements taken during a field campaign conducted in central California. We adapt the busy-time estimation methodology of Allen et al.<sup>20</sup> to account for recent changes in the ATOFMS data acquisition procedure. We advance the APS scaling methodology of Moffet et al.<sup>24</sup> by utilizing composition-dependent density values to obtain quantitative mass concentrations. We present the first evaluation of scaled ATOFMS mass concentrations against multiple, independent, co-located PM<sub>2.5</sub> measurement devices. These scaling approaches will be used for future ambient studies to obtain quantitative ATOFMS mass concentrations and can be applied to other SPMS measurements.

## EXPERIMENTAL SECTION

As part of the California Regional Particulate Air Quality Study (CRPAQS), two ATOFMS instruments were operated continu-

ously, sampling ambient aerosols from November 30, 2000, to February 4, 2001. The two sampling sites were an urban site in Fresno and a rural site in Angiola, both of which are located in central California.<sup>26</sup> Single particle size and chemical composition information on more than 2 million particles was acquired at each site. ATOFMS data are scaled with MOUDI (MSP Corp.) measurements at Fresno and with APS (TSI 3320) measurements at Angiola to obtain quantitative information. Other PM<sub>2.5</sub> measurements are also used for comparison and evaluation, including a beta attenuation monitor (BAM, Met One BAM 1020), tapered element oscillating microbalance (TEOM, Rupprecht & Patashnick TEOM 1400A), dust aerosol monitor (TSI DustTrak 8520), nephelometer (Radiance Research M903), and aethalometer (Magee Scientific RTAA1000). Only the measurements taken from January 9, 2001, to February 4, 2001 are presented in this work, representing 711 289 particles in Fresno and 614 915 particles in Angiola.

**ATOFMS Data Acquisition.** The design and operating principles of ATOFMS have been described in detail elsewhere,<sup>27</sup> and thus, we provide only a brief overview here. Particles enter the vacuum system through a converging nozzle, after which they are accelerated to terminal velocities that depend on their aerodynamic diameters, with larger particles traveling more slowly than smaller particles. Particles then enter a sizing region, where they intercept two continuous wave laser beams (diode pumped Nd:YAG at 532 nm) located 6 cm apart. Two scattering signals are collected as each particle passes through the two laser beams. Particle velocity can be calculated using the distance between the two laser beams and the time difference between the two scattering signals. These values are compared with an external calibration curve generated using monodisperse polystyrene latex spheres of known size. Using this curve, particle velocity can be converted into aerodynamic diameter. This velocity is also used to calculate the exact time when the particle arrives at the center of the ionization region. A 266-nm Nd:YAG ionization laser is triggered to fire upon particle arrival in the ion source region, and both positive and negative ions are analyzed by a dual polarity time-of-flight mass spectrometer. Thus, information on both single particle size and chemical composition can be acquired. Due to differences in the particle trajectories between the light scattering and ion source regions, not all particles that are sized produce a corresponding mass spectrum. Particles that produce both aerodynamic diameters and mass spectra are called hit particles, whereas particles that yield only aerodynamic diameters are called missed particles. A special ATOFMS operating condition is the fast scatter mode. When operating under this condition, ATOFMS records only missed particle size information without attempting to acquire mass spectra. Fast scatter measurements were occasionally used for obtaining overall particle size distribution.

After the field study, an in-house software program was used to calibrate the mass spectra and make a list of the individual ion peaks for each particle. These peak lists were then imported into a SPMS data analysis tool YAADA, for further analysis.<sup>28</sup>

- (16) Mansoori, B. A.; Johnston, M. V.; Wexler, A. S. *Anal. Chem.* **1994**, *66*, 3681–3687.
- (17) Gross, D. S.; Galli, M. E.; Silva, P. J.; Prather, K. A. *Anal. Chem.* **2000**, *72*, 416–422.
- (18) Reilly, P. T. A.; Lazar, A. C.; Gieray, R. A.; Whitten, W. B.; Ramsey, J. M. *Aerosol Sci. Technol.* **2000**, *33*, 135–152.
- (19) Bhave, P. V.; Allen, J. O.; Morrical, B. D.; Fergenson, D. P.; Cass, G. R.; Prather, K. A. *Environ. Sci. Technol.* **2002**, *36*, 4868–4879.
- (20) Allen, J. O.; Bhave, P. V.; Whiteaker, J. R.; Prather, K. A. *Aerosol Sci. Technol.* **2006**, *40*, 615–626.
- (21) Allen, J. O.; Fergenson, D. P.; Gard, E. E.; Hughes, L. S.; Morrical, B. D.; Kleeman, M. J.; Gross, D. S.; Galli, M. E.; Prather, K. A.; Cass, G. R. *Environ. Sci. Technol.* **2000**, *34*, 211–217.
- (22) Wenzel, R. J.; Liu, D. Y.; Edgerton, E. S.; Prather, K. A. *J. Geophys. Res. [Atmos.]* **2003**, *108*, 8427.
- (23) Sodeman, D. A.; Toner, S. M.; Prather, K. A. *Environ. Sci. Technol.* **2005**, *39*, 4569–4580.
- (24) Moffet, R. C.; Shields, L. G.; Bernsten, J.; Devlin, R. B.; Prather, K. A. *Aerosol Sci. Technol.* **2004**, *38*, 1123–1137.
- (25) Lake, D. A.; Tolocka, M. P.; Johnston, M. V.; Wexler, A. S. *Environ. Sci. Technol.* **2003**, *37*, 3268–3274.

- (26) Watson, J. G.; Chow, J. C.; Bowen, J. L.; Lowenthal, D. H.; Hering, S.; Ouchida, P.; Oslund, W. J. *Air Waste Manage. Assoc.* **2000**, *50*, 1321–1334.
- (27) Gard, E.; Mayer, J. E.; Morrical, B. D.; Dienes, T.; Fergenson, D. P.; Prather, K. A. *Anal. Chem.* **1997**, *69*, 4083–4091.
- (28) Allen, J. O. *Arizona State University*, 2002; <http://www.yaada.org>.

**MOUDI Measurements.** The MOUDI is based on particle impaction and has been extensively used for obtaining size-resolved particle mass and composition measurements.<sup>29</sup> During the CRPAQS, MOUDI data were collected at Fresno during six intensive operating periods (IOPs) within the time of interest for this study: 31 January 1000–1600, 1 February 0500–1000, 2 February 0000–0500, 2 February 1000–1600, 3 February 0500–1000, and 3 February 1600–2400. Angiola MOUDI measurements were not used in this study, since we were unable to accurately estimate ATOFMS busy time at that site due to a change in the data acquisition hardware in the middle of the study period.

**APS Measurements.** The APS provides information on both single particle number concentrations and  $D_a$  via light scattering and time-of-flight measurements.<sup>30</sup> It detects particles in the size range of 0.3–20  $\mu\text{m}$ , with accurate size-resolved counting of particles with  $D_a$  between 0.5 and 20  $\mu\text{m}$ . APS measurements were not collected at Fresno during the CRPAQS. At Angiola, measurements were obtained with a commercial APS (TSI 3320, Minnesota) from December 1, 2000, to February 4, 2001, with a temporal resolution of 5 min. The APS data were averaged over 1-h time periods. These hourly data are used in the scaling procedure described below.

## RESULTS AND DISCUSSION

**Scaling with MOUDI.** Previous investigations have shown that by comparing co-located ATOFMS and MOUDI data, quantitative information on particle mass concentrations can be acquired from ATOFMS measurements.<sup>20,21</sup> The advantage of scaling with MOUDI measurements is that they provide information on not only size-segregated total particle mass concentrations but also the size-segregated concentrations of individual chemical species that allow the derivation of ATOFMS relative sensitivity factors to different chemical species.<sup>19</sup> The disadvantage is that MOUDI samples are analyzed offline and provide coarse temporal- and size-resolution data. In this work, we adapt and modify the busy time estimation method developed by Allen et al.<sup>20</sup> and use it to scale the Fresno ATOFMS dataset with MOUDI measurements.

**ATOFMS Busy Time.** Busy time ( $t_b$ ) is defined as the amount of time that an ATOFMS instrument cannot detect incoming particles because it is busy processing data from a particle that just arrived. Previous studies revealed that three parameters are needed to compute ATOFMS instrument busy time: the time required to record a missed particle ( $A$ ), the time required to record the first hit particle in a folder ( $B$ ), and the incremental increase in time required to save each subsequent hit particle in a folder ( $C$ ). Laboratory experiments have been conducted to estimate these parameters, but when lab-based parameters are applied to field data, the results are at times not physically meaningful (e.g., busy time occasionally exceeds total sampling time). Thus, empirical methods have been developed to estimate busy time directly from field data. During the 1999 Bakersfield Instrument Intercomparison Study (BIIS), the ATOFMS instrument was operated alternately in normal data collection mode and fast scatter mode. Allen et al.<sup>20</sup> used data collected in fast scatter mode to estimate particle arrival rates ( $\lambda$ ). They demonstrated

that Poisson with busy time (PBT) distributions in conjunction with  $\lambda$  values can be used to compute  $A$  and that this information in combination with the particle data collected in normal operating mode can be used to compute  $B$  and  $C$ .

During CRPAQS and subsequent field campaigns, ATOFMS instruments were not routinely operated in fast scatter mode, so the methodology of Allen et al.<sup>20</sup> cannot be applied directly. In the present study, we adapt the previous methodology to estimate busy time parameters for the ATOFMS instrument that was stationed at Fresno. An analysis of the Fresno data set reveals five discrete time periods when the rate of missed particle detection ( $r_m$ ) doubled while the hit particle detection rate ( $r_h$ ) dropped substantially: 16 January 2150 to 17 January 0200, 28 January 0335–1115, 31 January 0430–0845, 1 February 0750–1040, and 2 February 0610–1000. As an example, Figure 1a illustrates the time series of  $r_m$  and  $r_h$  in 6-min intervals throughout 28 January. Several possible reasons for these “high-miss periods” were explored, but a definitive conclusion was not obtained. Nevertheless, even without a full understanding, it was determined that the data from these high-miss periods may be exploited to calculate  $A$ . The strong anticorrelations between  $r_m$  and  $r_h$  suggest that the busy time associated with missed particles caused the hit rate to drop during each high-miss period. Assuming that the degree to which  $r_h$  drops during the high-miss periods is determined by the time remaining to record hit particles after all missed particles are recorded,

$$\frac{N_{\text{Hit}}}{N_{\text{EstHit}}} = \frac{t - (AN_{\text{Missed}})}{t - (AN_{\text{EstMissed}})} \quad (1)$$

where  $t$  is the length of each sampling interval,  $N_{\text{Hit}}$  and  $N_{\text{Missed}}$  are the number of hit and missed particles recorded during a sampling interval, and  $N_{\text{EstHit}}$  and  $N_{\text{EstMissed}}$  are the estimated number of hit and missed particles if the high-miss event had not occurred. As illustrated in Figure 1a,  $N_{\text{EstHit}}$  and  $N_{\text{EstMissed}}$  are calculated in 6-min intervals by linear interpolation of  $r_h$  and  $r_m$ , respectively, over each high-miss period. By solving eq 1 for  $A$ , we obtain

$$A = \frac{t(N_{\text{Hit}} - N_{\text{EstHit}})}{(N_{\text{Hit}}N_{\text{EstMissed}}) - (N_{\text{EstHit}}N_{\text{Missed}})} \quad (2)$$

The values of  $A$  calculated during 6-min time intervals within each high-miss period are plotted against  $r_m$  in Figure 1b. The five different colors in Figure 1b represent results from different high-miss periods. As can be seen, there is remarkable consistency in the values of  $A$  across all five high-miss periods when  $r_m$  exceeds 2.5 Hz. These time intervals occurred at the peak of each high-miss period, when the instrument was devoting the vast majority of the sampling time to detecting missed particles. Thus, the  $A$  values calculated during these times are most robust. Whether setting the minimum  $r_m$  thresholds at 2.0, 2.5, 3.0, or 3.5 Hz, the mean value of  $A$  remains fairly constant at 0.26 s, with the standard deviation  $< 0.05$  s. On the basis of the above inspection, we use 3.0 Hz as the minimum  $r_m$  threshold, since at this frequency,  $A$  values are quite robust, and some data from all

(29) Marple, V.; Rubow, K.; Ananth, G.; Fissan, H. J. *J. Aerosol Sci.* **1986**, *17*, 489–494.

(30) Wilson, J. C.; Liu, B. Y. H. *J. Aerosol Sci.* **1980**, *11*, 139–150.

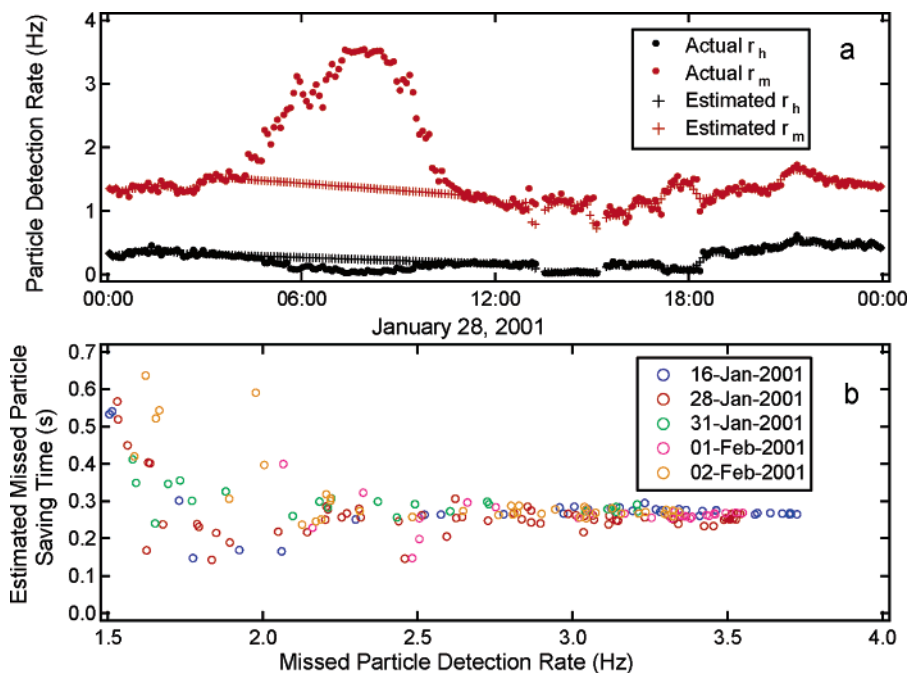


**Figure 1.** (a) Linear interpolation during the Fresno high-miss period to obtain estimated hit and missed counts for the period of January 28, 3:35–11:15; (b) estimated missed particle recording time vs missed particle detection rate for all five high-miss periods with a time resolution of 6 min for the Fresno dataset.

five high-miss periods are included. We therefore conclude that  $A = 0.264 \pm 0.013$  s. Note that the standard deviation is less than 5% of the mean  $A$  value.

PBT distributions using  $A = 0.264$  are used to estimate  $\lambda$  throughout the study period by following the procedure of Allen et al. in reverse order.<sup>20</sup> Excluding the high-miss periods when the application of PBT distributions is not justified, hourly  $\lambda$  values range between 0.11 and 15.1 Hz, with an average of 3.5 Hz. The best-fit  $B$  and  $C$  values are also calculated according to Allen et al.,<sup>20</sup> but the  $C$  value is not statistically significant due to smaller folder limits used during the CRPAQS (500 spectra/folder) relative to the BIIS (1000). We use our best-fit  $B$  value of 0.264 s and a  $C$  value of 0.00024 s taken from laboratory experiments conducted under similar conditions (H. Furutani, Personal Communication). The difference between the  $A$  values from this study and those from previous studies is attributed to a change in the ATOFMS data acquisition mode. ATOFMS can be operated in either nonwide dynamic range (non-WDR) or wide dynamic range (WDR) data acquisition mode.<sup>31</sup> When connecting two identical digitizers via a signal splitter to the signal source and attenuating one digitizer (30 db), WDR mass spectra (signal level ranging from 0 to 8000 instead of 0 to 255) can be obtained by combining the two signals.<sup>32</sup> Although operating ATOFMS in WDR mode produces mass spectra with a much greater dynamic range, it requires significant computer time and significantly increases both the  $A$  and  $B$  values. During the current study in Fresno, WDR spectra were acquired for positive ions, leading to a value of  $A$  that is higher than that in previous work when only non-WDR spectra were acquired.<sup>20</sup> The lab experiments also support our conclusion that  $A$  and  $B$  are comparable when operating in WDR mode, since the most time-consuming process in obtaining single

particle data is the data transfer from the acquisition board to the computer; the actual data-saving time represents only a minor fraction of the data transfer process.

*Scaling ATOFMS Measurements with MOUDI Measurements.* Scaled mass concentrations are calculated on the basis of the effective sampling duration, which excludes instrument busy time and offline periods. After obtaining ATOFMS busy time parameters, ATOFMS hit and missed particle information was processed for comparison with the MOUDI measurements. Hit particles were binned into size and time bins matching the MOUDI data. The MOUDI size bins are 0.18–0.32, 0.32–0.56, 0.56–1.00, and 1.00–2.50  $\mu\text{m}$ . The time frame is limited to the six MOUDI IOPs listed above. A total of 24 time–size bins are considered in the comparison, but data from two bins are excluded from the scaling procedure for the following reasons: (a) the MOUDI mass concentration was less than twice the mass uncertainty in the 1.00–2.50- $\mu\text{m}$  bin on 31 January 1000–1600, indicating high uncertainty in the MOUDI measurement; and (b) the total number of hit particles by ATOFMS in the 0.18–0.32- $\mu\text{m}$  bin on 1 February 0500–1000 was <100, which is deemed too few for a statistically representative measurement. Ultimately, mass concentrations in 22 bins were compared for quantitative analysis. Single particle sizes and counts were collected for each bin within the specified size range and time range. Using the measured flow rate through the instrument, an ATOFMS total particle mass concentration was calculated for each bin, assuming all the particles were spherical. Morawska and co-workers obtained an overall average ambient submicrometer particle density of 1.7  $\text{g}\cdot\text{cm}^{-3}$ .<sup>33</sup> The average density of supermicrometer particles would be even higher due to the increased fraction of sea salt and dust particles, which have densities of 1.9 and 2.7  $\text{g}\cdot\text{cm}^{-3}$ , as reported by Hänel and

(31) Dienes, T. Ph.D. Thesis, University of California, Riverside, 2003.

(32) Beavis, R. C. *J. Am. Soc. Mass Spectrom.* **1996**, *7*, 107–113.

(33) Morawska, L.; Johnson, G.; Ristovski, Z. D.; Agranovski, V. *Atmos. Environ.* **1999**, *33*, 1983–1990.

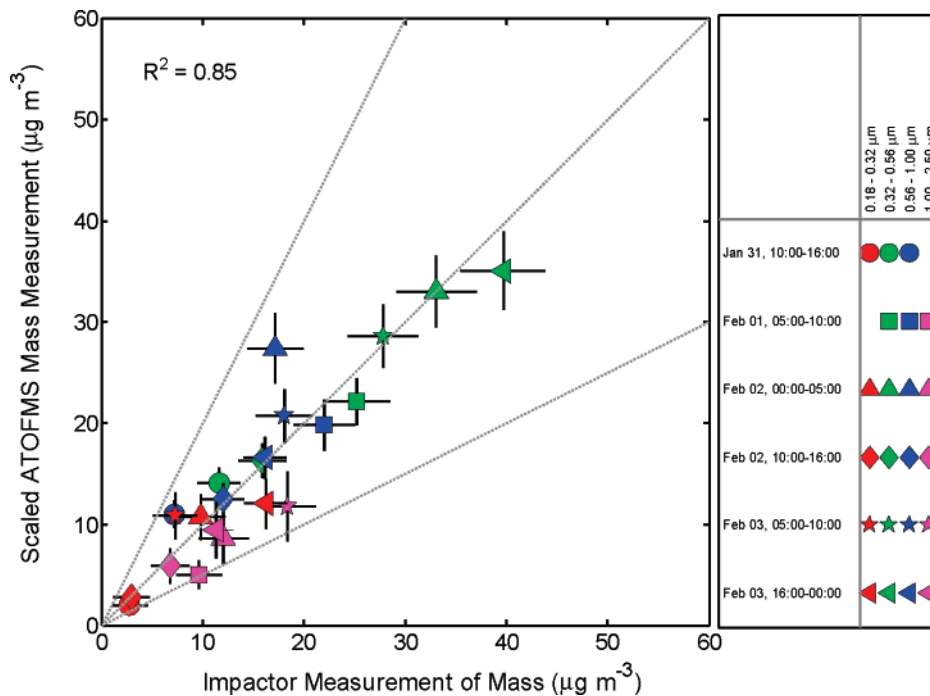


**Figure 2.** Comparison of scaled ATOFMS and MOUDI mass concentrations in Fresno.

Thudlum.<sup>34</sup> Thus, we use a density of  $1.9 \text{ g}\cdot\text{cm}^{-3}$  for all  $\text{PM}_{2.5}$  particles in mass concentration calculation instead of the  $1.3 \text{ g}\cdot\text{cm}^{-3}$  value used in previous work.<sup>19–21,35</sup> The scaling factor,  $\phi_{\text{MOUDI}}$ , was constructed as the parameter to compensate for the difference between ATOFMS and MOUDI measurements.  $\phi_{\text{MOUDI}}$  represents the inverse of the ATOFMS particle detection efficiency and is defined using the following expression,

$$\phi_{\text{MOUDI}} = \frac{m_{\text{MOUDI}}}{m_{\text{ATOFS}}} \quad (3)$$

where  $m_{\text{MOUDI}}$  is the MOUDI mass concentration, and  $m_{\text{ATOFS}}$  is the ATOFMS mass concentration before scaling.  $\phi_{\text{MOUDI}}$  is a function of particle size and can be expressed with a power law relationship with  $D_a$ ,

$$\phi_{\text{MOUDI}} = \alpha D_a^\beta \quad (4)$$

where  $\alpha$  and  $\beta$  are the best-fit parameters determined by nonlinear regression of  $m_{\text{MOUDI}}$  on  $m_{\text{ATOFS}}$  over all 22 bins. Physically,  $1/\alpha$  is the particle detection efficiency for a  $1.0\text{-}\mu\text{m}$  particle, and  $\beta$  represents the degree to which particles with suboptimal sizes are deflected from the centerline in the ATOFMS inlet. On the basis of eq 4, it is clear that varying the density value will not affect the scaled results; only the scaling parameters will change. For this study, the best-fit values of  $\alpha$  and  $\beta$  are  $1748 \pm 364$  and  $-4.41 \pm 0.28$ , respectively, so  $\phi_{\text{MOUDI}}$  varies from  $3.4 \times 10^6$  for a  $0.18\text{-}\mu\text{m}$  particle to 31 for a  $2.5\text{-}\mu\text{m}$  particle.

Upon obtaining  $\alpha$  and  $\beta$ , the value of  $\phi_{\text{MOUDI}}$  was calculated for every single particle using eq 4 on the basis of the measured

particle diameters by ATOFMS. The following equation was used to calculate scaled ATOFMS mass concentrations,

$$m_{\text{ATOFS-MOUDI}} = \sum_i \phi_{D_{a,i}} m_i \quad (5)$$

where  $m_{\text{ATOFS-MOUDI}}$  is the ATOFMS mass concentration after scaling with MOUDI, and  $\phi$  and  $m_i$  are the scaling factors and mass concentrations for each single particle, respectively. Comparison of the scaled ATOFMS and the MOUDI mass concentrations for all 22 bins results in an  $R^2$  value of 0.85, as shown in Figure 2, indicating that two parameters ( $\alpha$  and  $\beta$ ) are sufficient to explain 85% of the variability in ATOFMS transmission efficiencies over the  $0.18\text{--}2.5\text{-}\mu\text{m}$   $D_a$  range during six different IOPs. It is important to note that the high  $R^2$  value would not have been obtained if busy-time corrections had not been applied. Note the mass concentrations for the non-IOP periods can be calculated with the same scaling function at higher temporal resolution (1 h) if one assumes that the ATOFMS scaling factors do not change over time. There is some uncertainty associated with this assumption, so scaling with real-time particle concentration measurements may be favorable for obtaining total mass concentrations, as described in the next section.

*Comparison between MOUDI Scaled ATOFMS Measurements and BAM Measurements.* Both hourly BAM and hourly TEOM  $\text{PM}_{2.5}$  mass measurements were made at the Fresno site. Because the TEOM inlet was heated to  $50 \text{ }^\circ\text{C}$  during sampling to remove interferences from water, other semivolatile compounds were also removed,<sup>36</sup> yielding values that were systematically lower than the co-located BAM measurements by an average of 42%. Therefore, since ATOFMS does not remove water or semivolatile compounds

(34) Hänel, G.; Thudium, J. *Pure Appl. Geophys.* **1977**, *115*, 799–803.

(35) Pastor, S. H.; Allen, J. O.; Hughes, L. S.; Bhave, P.; Cass, G. R.; Prather, K. A. *Atmos. Environ.* **2003**, *37*, S239–S258.

(36) Charron, A.; Harrison, R. M.; Moorcroft, S.; Booker, J. *Atmos. Environ.* **2004**, *38*, 415–423.

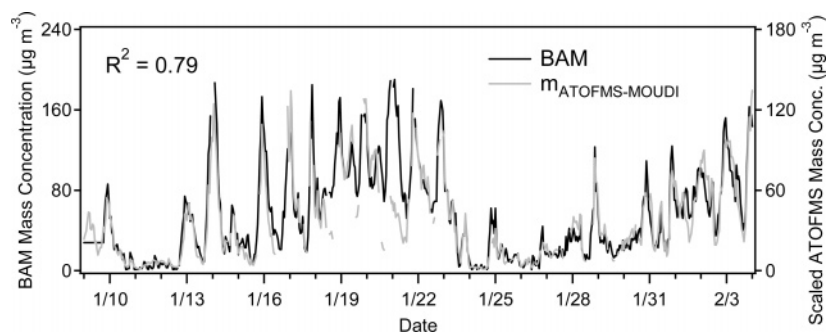


**Figure 3.** Temporal variations of hourly BAM and scaled ATOFMS PM<sub>2.5</sub> mass concentrations in Fresno. The scaling function for the ATOFMS was obtained by comparison with MOUDI measurements.

to a significant extent due to short analysis times, hourly BAM mass concentration measurements ( $m_{\text{BAM}}$ ) were chosen as the reference mass concentration to evaluate  $m_{\text{ATOFMS-MOUDI}}$  for the entire study period, as shown in Figure 3. Both mass concentration measurements show distinct diurnal temporal variations, reaching maximums and minimums at nearly the same time each day. Particulate matter concentrations remained relatively low during the day and increased substantially at night in Fresno during this study. The correlation between  $m_{\text{BAM}}$  and  $m_{\text{ATOFMS-MOUDI}}$  is notably high, with an  $R^2$  value of 0.79. However, Figure 3 also shows that  $m_{\text{ATOFMS-MOUDI}}$  is systematically lower ( $\sim 30\%$  less) than  $m_{\text{BAM}}$ . The ratio of mean values between these two measurements is 0.69 over the 26-day sampling period of interest. Several factors account for this difference. First, particles below  $0.20 \mu\text{m}$  are not included in the  $m_{\text{ATOFMS-MOUDI}}$  value because this represents the lowest size detectable by the ATOFMS instrument used in this study. An analysis of the MOUDI data during the six IOPs of interest indicates that particles larger than  $0.18 \mu\text{m}$  make up 86% of the total PM<sub>2.5</sub> mass summed over all impaction stages from 0 to  $2.5 \mu\text{m}$  ( $\Sigma m_{\text{MOUDI}}$ ). Second, the mean value of  $m_{\text{MOUDI}}$  during the six IOPs is only 88% of the mean value of  $m_{\text{BAM}}$ . These two factors alone make it so the value of  $m_{\text{ATOFMS-MOUDI}}$  cannot exceed 76% of the  $m_{\text{BAM}}$  value ( $0.86 \times 0.88 = 0.76$ ). Furthermore, the scaling function derived from the six IOPs may have varied during the 26-day period. Thus, these factors result in the absolute values of  $m_{\text{ATOFMS-MOUDI}}$  being 30% lower than the  $m_{\text{BAM}}$  values.

**Scaling with the APS.** *Scaling ATOFMS Measurements with APS Measurements.* Another quantification approach involves comparison of the ATOFMS particle counts at Angiola with particle number concentrations acquired with a co-located APS. Although APS measurements are not able to provide mass concentrations of individual chemical species, such as the MOUDI, they can provide particle number concentrations with very high temporal and size resolutions. These high-resolution reference data can potentially provide more accurately scaled ATOFMS mass concentrations.

To scale the ATOFMS data with APS measurements, we follow an approach similar to the MOUDI scaling method by deriving scaling functions to correct for ATOFMS particle undercounting. To take advantage of the high time resolution properties of both measurements, one scaling function was constructed for each hour of the entire study period. Within each hour, single particle number counts collected by both ATOFMS and APS were segregated into 12 size ranges:  $0.300\text{--}0.523$ ,  $0.523\text{--}0.605$ ,  $0.605\text{--}0.699$ ,  $0.699\text{--}0.807$ ,  $0.807\text{--}0.933$ ,  $0.933\text{--}1.077$ ,  $1.077\text{--}1.243$ ,  $1.243\text{--}$

$1.435$ ,  $1.435\text{--}1.655$ ,  $1.655\text{--}1.911$ ,  $1.911\text{--}2.207$ , and  $2.207\text{--}2.547 \mu\text{m}$ . These size bins were adapted directly from the APS size bins by combining pairs of adjacent bins between  $0.523$  and  $2.547 \mu\text{m}$  so that high hourly ATOFMS hit particle counts could be obtained for each bin. The smallest APS bin ( $0.300\text{--}0.523 \mu\text{m}$ ) is also included in this calculation. When the smallest APS bin is not used, the results do not change substantially from the 12-bin scaling discussed below. Since scaling is performed hourly, the factors that affect ATOFMS sampling, such as busy time and instrument offline time, are accounted for implicitly. The scaling factor,  $\phi_{\text{APS}}$ , is defined as the following:

$$\phi_{\text{APS}} = \frac{\text{Count}_{\text{APS}}}{\text{Count}_{\text{ATOFMS}}} \quad (6)$$

One scaling factor was acquired for each size bin with eq 6 for each hour. Like the scaling factors used in MOUDI scaling,  $\phi_{\text{APS}}$  is also size-dependent. By plotting the scaling factors against  $D_a$ , a scaling curve can be constructed for particles with aerodynamic diameters below  $2.5 \mu\text{m}$ . Figure 4a shows the hourly scaling curves for the ATOFMS instrument stationed at Angiola on February 3. The error bars are generally not significant, except for those at 5:00 and 6:00, during which APS measurements showed variations. The instrument was offline between 13:00 and 14:00, and therefore, no scaling curve for this time period is presented. In Figure 4a, we see that  $\phi_{\text{APS}}$  varies substantially from hour to hour. In the largest size bin, this variation spans nearly 1 order of magnitude. Most of this variability results from differences in ambient particle concentrations, leading to differences in instrument busy times.<sup>23</sup> This result further emphasizes the importance of high time resolution (hourly) scaling. The scaling factors obtained with MOUDI measurements will not be as accurate as  $\phi_{\text{APS}}$  due to the time and size resolution limit and may not be able to reflect short-term ambient particle concentration changes. In general, the APS scaling curve reaches a minimum at the  $1.655\text{--}1.911 \mu\text{m}$  size bin (bin midpoint is  $1.783 \mu\text{m}$ ) due to the higher ATOFMS transmission efficiency of particles in this size range than others. Two scaling functions were obtained for each hour by fitting the scaling curve separately on each side of the minimum point. Examples of the fitting of the scaling curve are included in Figure 4b and c for 22:00 on February 03, 2001. The scaling function for the size range of  $1.783 \mu\text{m}$  and below was obtained by exponential regression and was extrapolated down to  $0.2 \mu\text{m}$  to obtain the scaling factors for the smallest

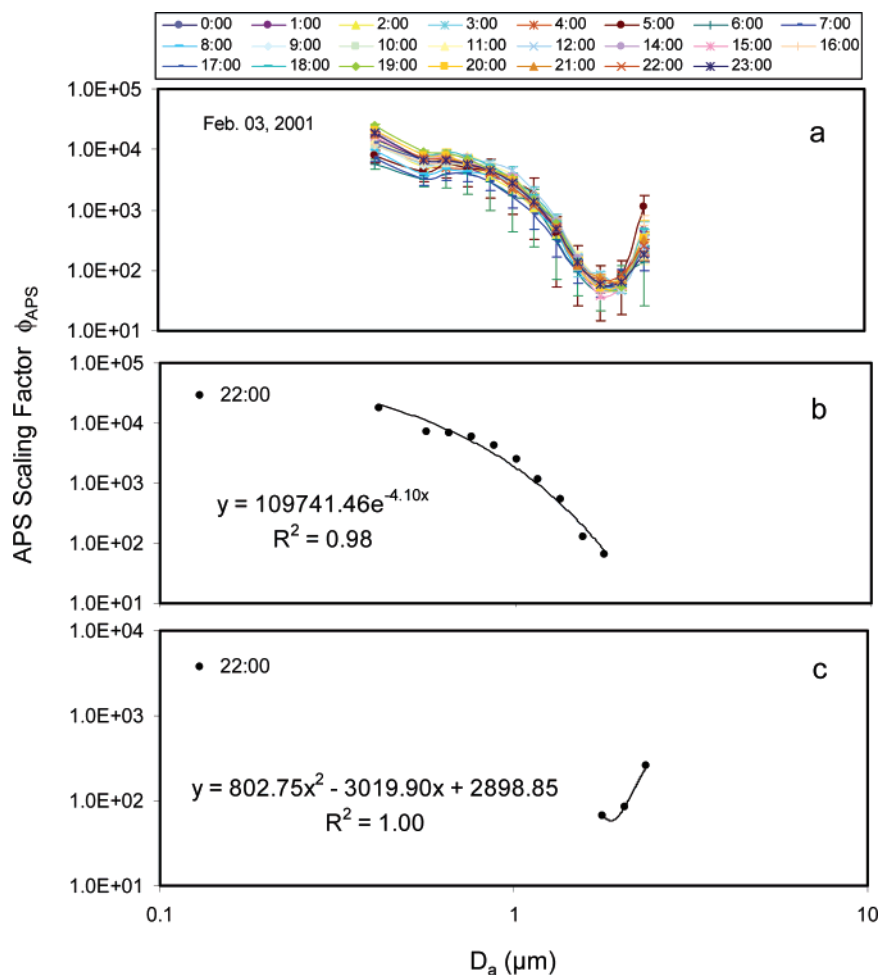


**Figure 4.** APS scaling curve for Angiola measurements: (a) hourly scaling curve for February 03, except for 13:00; (b) exponential regression of left half of scaling curve at 22:00; (c) polynomial regression of right half of scaling curve at 22:00.

particles detected by ATOFMS. The scaling function for the size range above  $1.783 \mu\text{m}$  was obtained by a second-order polynomial regression. Thus, each scaling function can be fully described with five parameters that are used to calculate  $\phi_{\text{APS}}$ , as shown in eq 7:

$$\phi_{\text{APS}} = \begin{cases} C_1 e^{C_2 \cdot D_a} & (\text{when } D_a < 1.783 \mu\text{m}) \\ C_3 D_a^2 + C_4 D_a + C_5 & (\text{when } D_a \geq 1.783 \mu\text{m}) \end{cases} \quad (7)$$

Five parameters were obtained for each hour of data collected at Angiola to correct ATOFMS measurements with APS measurements, generating number concentrations with 1-h temporal resolution. The form of eq 7 will allow a similar relationship to be applied to other studies to obtain APS scaling factors.

With the resulting scaling functions, quantitative ATOFMS mass concentrations ( $m_{\text{ATOFMS-APS}}$ ) were calculated. The  $\phi_{\text{APS}}$  value for each particle can be obtained using the measured  $D_a$  and the time when each data point was acquired.  $m_{\text{ATOFMS-APS}}$  is calculated with the following equation, knowing the instrument nozzle flow rate and assuming the particles were spherical,

$$m_{\text{ATOFMS-APS}} = \sum_i \frac{M(D_{a,i}) \phi_{\text{APS}}(D_{a,i})}{V_{\text{ATOFMS}}} \quad (8)$$

where  $M(D_{a,i})$  is the mass of each particle and  $V_{\text{ATOFMS}}$  is the volume of flow within each time period. Equation 8 makes it possible to construct quantitative particle mass concentrations for individual particle classes with any size and temporal resolution. Unlike MOUDI scaling,  $m_{\text{ATOFMS-APS}}$  is sensitive to assumed particle density values. Rather than assuming all particles have the same density, we may assign different densities to particles with different chemical compositions for improved estimates of the total mass concentrations.

*Comparison between BAM Measurements and APS Scaled ATOFMS Mass Concentrations Obtained with Different Density Values.* The most straightforward approach to obtaining mass concentrations from ATOFMS data is to assign a single density value to all particles. Figure 5a shows the correlation between  $m_{\text{BAM}}$  and  $m_{\text{ATOFMS-APS}}$  when utilizing fixed density values of 1.8, 1.9, and  $2.0 \text{ g}\cdot\text{cm}^{-3}$ , respectively, for APS scaling. The slope of each regression represents the ratio of mean values between  $m_{\text{BAM}}$  and  $m_{\text{ATOFMS-APS}}$ . The value for  $m_{\text{ATOFMS-APS}}$  shows the best agreement with  $m_{\text{BAM}}$  when utilizing a density of  $1.9 \text{ g}\cdot\text{cm}^{-3}$  (shown in red in Figure 5a). The temporal variations of the above two mass concentrations are presented in Figure 6. They track each other extremely well, with an  $R^2$  value of 0.91. The Angiola particles were highly aged and dominated by carbonaceous species as well as significant quantities of nitrate and ammonium,

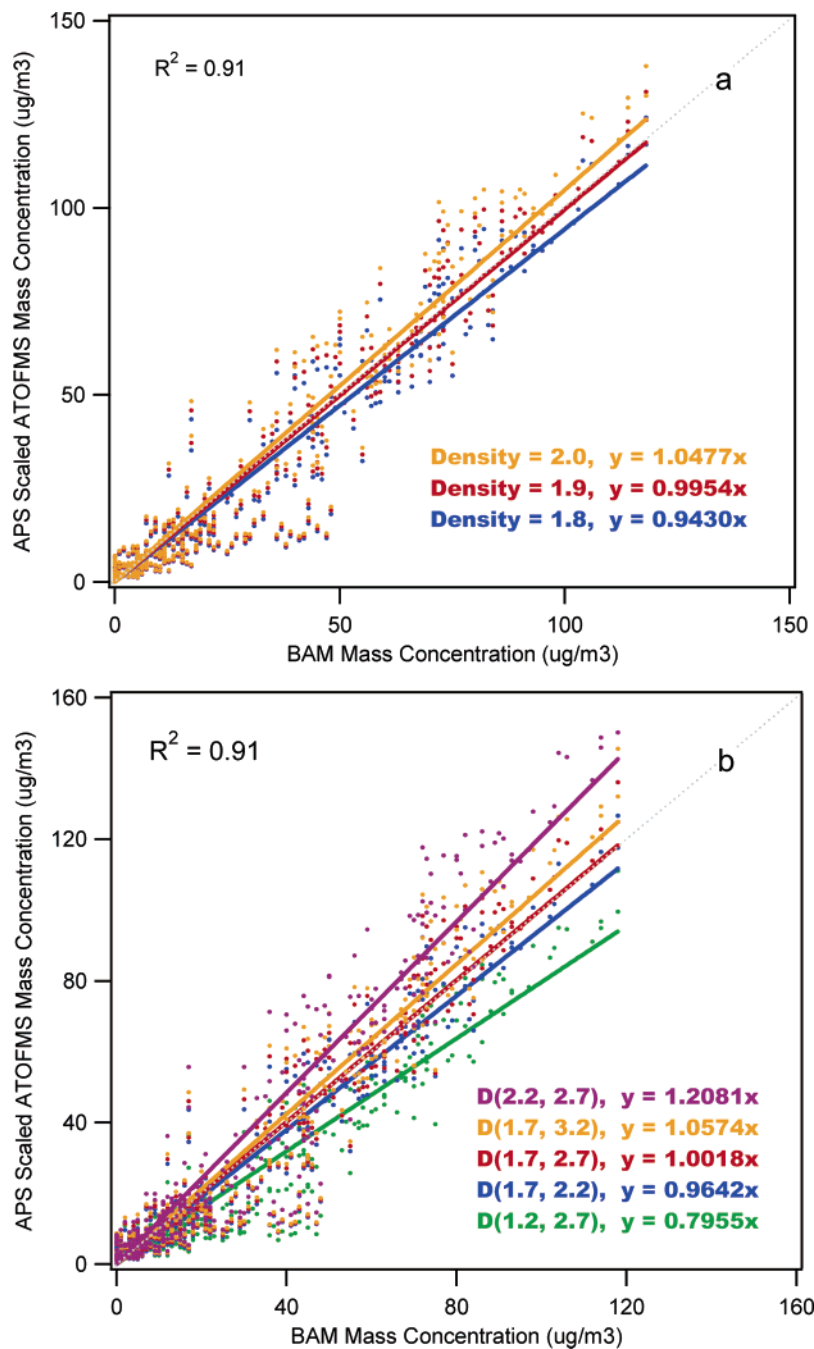


**Figure 5.** Correlations between BAM and APS scaled ATOFMS mass concentrations. (a) ATOFMS mass concentrations are obtained with single density ( $\rho$ ) values for all particles ( $\rho = 1.8, 1.9, \text{ or } 2.0 \text{ g}\cdot\text{cm}^{-3}$ ); (b) ATOFMS mass concentrations are obtained with different density pairs for submicrometer and supermicrometer particles: 1.2 and 2.7; 1.7 and 2.2; 1.7 and 2.7; 1.7 and 3.2; and 2.2 and 2.7  $\text{g}\cdot\text{cm}^{-3}$ .

representing more than 80% of the total particles detected by ATOFMS. As particles age, they become internally mixed aerosols composed of organic carbon, ammonium, nitrate, sulfate, and water, and in general, the particle-to-particle chemical variability decreases over time. Thus, the good agreement between ATOFMS mass concentrations scaled with a single density and BAM measurements is consistent with the chemical homogeneity of aged ambient aerosols. When applying the above method to scale ATOFMS measurements in a region where fresh emissions occur and many distinct particle types dominate, it is likely that applying one density value for all particles will not be sufficient.

Since ATOFMS measures the aerodynamic diameters of individual particles, it is possible to apply specific density values

based on particle size. The unscaled ATOFMS ambient particle size distribution shows that particles with  $<1.0 \mu\text{m}$  account for a large portion of total particle numbers in Angiola. ATOFMS chemical composition measurements have shown that particles smaller than  $1.0 \mu\text{m}$  are mainly carbonaceous particles with associated secondary inorganic components, whereas the relative fraction of inorganic (i.e., sea salt, dust) particles increases substantially above  $1.0 \mu\text{m}$ .<sup>37</sup> Thus, we segregate particles into two size ranges: submicrometer ( $0.2 \leq D_a < 1.0 \mu\text{m}$ ) and supermicrometer ( $1.0 \leq D_a < 2.5 \mu\text{m}$ ). We use the literature value of  $1.7 \text{ g}\cdot\text{cm}^{-3}$  as the density for submicrometer particles,<sup>33</sup> and

(37) Noble, C. A.; Prather, K. A. *Environ. Sci. Technol.* **1996**, *30*, 2667–2680.

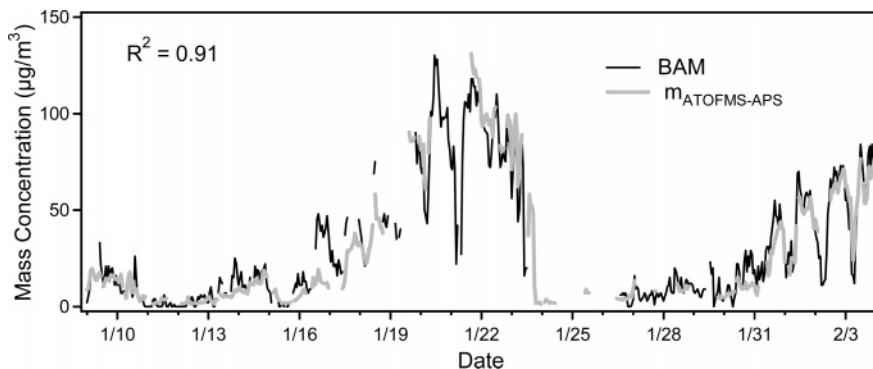


**Figure 6.** Temporal variation of Angiola particulate mass concentrations obtained with BAM and APS scaled ATOFMS ( $\rho = 1.9 \text{ g}\cdot\text{cm}^{-3}$ ).

$2.7 \text{ g}\cdot\text{cm}^{-3}$  for supermicrometer particles, an intermediate value for the various chemical components reported in this size range.<sup>34</sup> The scatter plot between  $m_{\text{ATOFMS-APS}}$  acquired with this pair of density values and  $m_{\text{BAM}}$  is included in Figure 5b (in red). Scaled ATOFMS and BAM mass concentrations track each other very well, with a high correlation coefficient of 0.91. The absolute values are quite close to one another and nearly on top of the 1:1 line. We also varied the densities by  $0.5 \text{ g}\cdot\text{cm}^{-3}$  in both directions for the sub- and supermicrometer particles separately. The correlations of BAM measurements with scaled ATOFMS data using each of these density pairs are also included in Figure 5b. The correlation values remain high ( $R^2 \sim 0.91$ ) in all cases, and only the ratios between  $m_{\text{ATOFMS-APS}}$  and  $m_{\text{BAM}}$  are different. From the change in slope, it is apparent that the total scaled ATOFMS mass concentrations are more sensitive to the submicrometer particle density than the supermicrometer particle density. This is due to the fact that the majority of the Angiola particle mass is in the submicrometer size mode.

We can go beyond just using size information and apply chemically specific density values to each different particle type to obtain scaled ATOFMS mass concentrations. To convert from number to mass concentrations, we used the density value of  $1.9 \text{ g}\cdot\text{cm}^{-3}$  for carbonaceous particles,  $2.7 \text{ g}\cdot\text{cm}^{-3}$  for dust particles,  $1.9 \text{ g}\cdot\text{cm}^{-3}$  for Na-rich salt particles,  $2.0 \text{ g}\cdot\text{cm}^{-3}$  for biomass emission particles and EC rich particles, and  $1.9 \text{ g}\cdot\text{cm}^{-3}$  for the rest of the particle types.<sup>34,38,39</sup> The multidensity scaled ATOFMS mass concentrations also show a strong and very similar correlation with BAM measurements, with a high  $R^2$  of 0.91. As discussed earlier in this section, the advantages of utilizing various density values for each chemical composition are not fully realized in this particular study due to the fact that Angiola ambient particles are aged and, thus, very chemically homogeneous. In regions or seasons with more fresh emissions, it will most likely become necessary to assign chemically specific density values for individual particle types. Additional lab and field investigations are underway to develop universal scaling factors that use specific density and shape factors for each particle type.

**PM<sub>2.5</sub> Measurement Intercomparison.** A number of different continuous particle measurements were available in both Fresno and Angiola during the CRPAQS. Thus, it is possible to compare the correlations among different measurements. Such

comparisons are helpful for evaluating the different methods used for scaling the ATOFMS mass concentrations. At the Fresno site, the available continuous PM<sub>2.5</sub> measurements are BAM, TEOM, DustTrak, nephelometer, aethalometer, and  $m_{\text{ATOFMS-MOUDI}}$ . Several hours of nephelometer data points were removed in the morning periods of January 30, January 31, and February 1 due to the extraordinarily high uncertainties in these measurements. The continuous PM<sub>2.5</sub> measurements for the Angiola site include BAM, nephelometer, aethalometer, and  $m_{\text{ATOFMS-APS}}$ , with density values of  $1.9 \text{ g}\cdot\text{cm}^{-3}$  for all particles. Although the measurements of all of these instruments represent the total PM<sub>2.5</sub> particle mass concentrations, each instrument is based on a different theory and has its own strengths and weaknesses. Therefore, it is quite reasonable to expect the correlation between any two measurements to be  $<1$ .<sup>40</sup>

The correlation coefficients between various pairs of measurements are tabulated in Table 1 for both Fresno and Angiola. For Fresno site comparisons, if one uses an  $R^2$  value of 0.7 and above to represent a good correlation, only the BAM measurement shows a fairly good correlation with all the other measurements, with correlation coefficients ranging from 0.75 to 0.93. The TEOM measurement correlates well only with BAM and aethalometer measurements. This suggests that in this environment, the heated TEOM does not provide measurements of mass concentrations that are as accurate as those of the BAM. The  $m_{\text{ATOFMS-MOUDI}}$  correlates well with the BAM, DAM, and nephelometer measurements. The overall correlation for MOUDI-scaled ATOFMS PM<sub>2.5</sub> mass concentrations are as close as most other PM<sub>2.5</sub> measure-

**Table 1. Correlation Coefficients of PM<sub>2.5</sub> Measurements**

Fresno $R^2$	BAM	TEOM	DAM	NEPH	AETH	ATOF-M <sup>a</sup>
BAM	1.00	0.86	0.93	0.75	0.79	0.79
TEOM	0.86	1.00	0.59	0.60	0.94	0.64
DAM	0.93	0.59	1.00	0.70	0.53	0.78
NEPH	0.75	0.60	0.70	1.00	0.58	0.81
AETH	0.79	0.94	0.53	0.58	1.00	0.62
ATOF-M	0.79	0.64	0.78	0.81	0.62	1.00
Angiola $R^2$	BAM	NEPH	AETH	ATOF-N <sup>b</sup>		
BAM	1.00	0.92	0.60	0.91		
NEPH	0.92	1.00	0.77	0.93		
AETH	0.60	0.77	1.00	0.63		
ATOF-N	0.91	0.93	0.63	1.00		

<sup>a</sup> MOUDI-scaled ATOFMS mass concentrations. <sup>b</sup> APS-scaled ATOFMS mass concentrations.

(38) McMurry, P. H.; Wang, X.; Park, K.; Ehara, K. *Aerosol Sci. Technol.* **2002**, *36*, 227–238.

(39) Pitz, M.; Cyrys, J.; Karg, E.; Wiedensohler, A.; Wichmann, H. E.; Heinrich, J. *Environ. Sci. Technol.* **2003**, *37*, 4336–4342.

ments in Fresno. Similarly, Angiola correlation comparisons are shown in Table 1. The BAM, nephelometer, and  $m_{\text{ATOFMS-APS}}$  measurements show high correlation coefficients of  $>0.90$ . The aethalometer measurements differ substantially and show lower correlation coefficients with the other three measurements. The strong correlation of ATOFMS mass concentrations with other  $\text{PM}_{2.5}$  measurements provides support that the ATOFMS data can be scaled using peripheral instruments, such as the APS, to provide a measure of real ambient particle mass concentrations. It is important to note that the ultimate goal in developing this scaling procedure is not to just provide total  $\text{PM}_{2.5}$  mass concentrations, since these can be measured using a variety of other dedicated techniques, but instead, to use ATOFMS to provide mass concentrations of particles from specific sources. Thus, this scaling and comparison study represents a critical step in the development of the most appropriate scaling procedures that will allow us to use ATOFMS to obtain quantitative source apportionment results in future studies.

## CONCLUSIONS

In this paper, we compare two methods for scaling ATOFMS measurements using reference measurements to obtain quantitative particle mass concentrations. By comparing ATOFMS single particle measurements with MOUDI mass measurements, we obtain scaled ATOFMS mass concentrations that correlate well ( $R^2 = 0.79$ ) with a BAM, which serves as an independent mass concentration reference method. However, the absolute values of scaled ATOFMS mass concentration are close to MOUDI measurements only during the IOPs within the specified size range. Reduced ratios between the scaled ATOFMS and BAM mass concentrations are obtained when applying the scaling function to other periods during the study. Increasing the time resolution of the scaled ATOFMS mass concentrations to 1 h (i.e., shorter than that of the MOUDI, which is 5–8 h) also introduces uncertainties. Both of these factors result in the absolute values of scaled ATOFMS mass concentration being only 70% of those measured by the BAM over the full study. Some of this difference can be explained by the underestimation of particles smaller than

$0.18 \mu\text{m}$  by ATOFMS. The main advantage of scaling with the MOUDI measurements is to obtain size-segregated mass concentrations of individual chemical species, making it possible to derive relative sensitivity factors.<sup>19</sup>

APS measurements provide high temporal resolution particle number concentrations. By scaling ATOFMS particle counts with the APS and applying composition specific density values to the ATOFMS particle types, we are able to obtain ambient particle mass concentrations that correlate extremely well with BAM measurements ( $R^2 = 0.91$ ). Future papers will address using chemically specific scaling factors which correct for density and shape factors.

In conclusion, continuous and quantitative ambient particle mass concentrations can be obtained from ATOFMS measurements by scaling with measurements from a co-located MOUDI or APS. The MOUDI method should be used if one is interested in deriving chemical sensitivity factors for different species. If one is more interested in real-time variations in particle mass concentrations (i.e., from different sources), the APS method is a more appropriate choice. The use of these methods for scaling extends ATOFMS to a more quantitative tool for studying ambient aerosol composition, transformations, and reaction mechanisms. When applying these scaling methods to individual particle types measured by the ATOFMS and correcting for chemical differences, quantitative mass concentrations of individual chemical (or source) types with high time and size resolution can be obtained.

## ACKNOWLEDGMENT

We thank the California Air Resources Board for financial support (Contract No. 04-336) and the SJV funding agency for supporting CRPAQS. We also thank Dr. Hiroshi Furutani for sharing his busy-time results and Dr. William Vance (CARB) and Prof. Jon Allen (ASU) for their thoughtful comments on this manuscript.

Received for review March 2, 2006. Accepted June 16, 2006.

AC060395Q

(40) Lee, J. H.; Hopke, P. K.; Holsen, T. M.; Polissar, A. V.; Lee, D. W.; Edgerton, E. S.; Ondov, J. M.; Allen, G. *Aerosol Sci. Technol.* **2005**, *39*, 261–275.